Int J Adv Manuf Technol (2017) 92:2545–2557
DOI 10.1007/s00170-017-0330-1

ORIGINAL ARTICLE

Numerical visualization and optimization on the core penetration in multi-cavity co-injection molding with a bifurcation runner structure

Chao-Tsai Huang[1]

Received: 3 November 2016 / Accepted: 22 March 2017 / Published online: 4 April 2017

Abstract Co-injection molding and multi-cavity molding are common processes for plastic products manufacturing. These two systems are sometimes combined and applied in the manufacture of bifurcation-structure products. However, how the influential factors truly affect the core penetration behavior and the detailed mechanism of core penetration behavior has not yet been fully understood. In this study, it has focused on studying the multi-cavity co-injection system with a bifurcation runner structure. The results showed that when the skin-to-core ratio is fixed (say 72/28), the melt flow behavior of a co-injection system, utilizing the same material for both skin and core, is very similar to that of a single shot injection molding. Specifically, the non-symmetrical bifurcation runner structure will influence the flow behavior greatly and cause the core distribution imbalance between different cavities. However, it is observed that when the flow rate is increased, the core material will occupy more volume space in the upstream portion of the runner and the core penetration distance will be reduced in the flow direction downstream. This feature is very useful to further manipulate the skin/core interface in a multi-cavity system. Moreover, regarding how to improve a poor inter-cavity balance of core material distribution, using a suitable adjustment of the skin-to-core ratio will be greatly helpful. However, the core break-through defect can be a common problem in co-injection molding when an unsuitable skin-to-core ratio is used. To prevent the core break-through defect, increasing the flow rate properly can be one of the good options that we can use. Hence, it is concluded that a suitable adjustment of the skin-to-core ratio and a proper flow rate control can be used to optimize the core material distribution in multi-cavity co-injection molding with a bifurcation runner structure. Lastly, in order to validate the inference and the effectiveness of this proposal to improve the inter-cavity imbalance and core break-through problem, a series of experimental studies were performed. And, all experimental results are in good agreement with those of our numerical predictions to further validate the feasibility of our proposed method to gain a better control of the core material distribution with a bifurcation runner structure in multi-cavity co-injection molding.

Keywords Co-injection molding · Core penetration · Skin-to-core ratio · Flow imbalance

✉ Chao-Tsai Huang
cthuang@mail.tku.edu.tw; cthuang@moldex3d.com

[1] Department of Chemical and Materials Engineering, Tamkang University, No. 151, Yingzhuan Rd., Tamsui Dist, New Taipei City 25137, Taiwan

1 Introduction

The demand for smart and lightweight technologies has become the driving force for the advanced product developments in the automotive and other industry sectors in recent years. One of the common weight-saving technologies used in the automotive industry is the application of short or long fiber-reinforced thermoplastics (FRT), replacing metal in many car components. However, it still encounters some challenges. For example, the fiber breakage during the manufacturing or how to catch the micro-structures of fibers is some of the crucial problems [1–3]. Furthermore, since thousands of plastics are made yearly, the recycling of plastics has already posed a serious environmental problem. One of the recycling methods used today is through a mechanical approach by shredding, crushing, milling, and then the reuse of plastics. This is a good recycling method, free of using any chemical or solvent; however, it has a poor control on the

microstructure of fibers. Thus, it will restrict this kind of recycled fiber content fillers to lower-profit applications only [4–6].

Moreover, co-injection molding has been developed and applied in many industry sectors for decades [7, 8]. Various skin/core material combinations, such as soft in skin/hard in core, raw in skin/reinforced in core, or fresh material in skin/recycled material in core, are commonly used in today's manufacturing world in products like automotive components and structural reinforcement parts. Some significant advantages of co-injection include cost reduction, reuse of materials, and excellent production efficiency. Generally speaking, the strength of structural reinforced products is determined by the skin/core material distribution. Hence, co-injection molding with a proper control of the skin/core distribution is one of the good solutions when handling recycled plastics with fiber contents. The relationships between the material distribution behavior with the process conditions, and/or material properties, are discussed in many previous research studies [9–11]. Currently, some researchers tried to develop a numerical method to catch the evolution of skin/core interface for sequential co-injection molding, but only in a single-cavity system [12]. However, in reality, it is very difficult to control the skin-to-core material ratio distribution especially when molding parts with a complex geometry. Although, several general guidelines for the co-injection process have been developed from the previous studies; however, they are still not sufficient enough to provide a clear understanding as to how to achieve a good core distribution.

Moreover, the multi-cavity co-injection molding process has been applied in the manufacture of bifurcation structure products such as window stripes or concept for plastic recycling [13, 14] and high-end furniture products [15]. The bifurcation structure can be seen in the geometric design of the runner in the mold or in the part design. Generally speaking, it

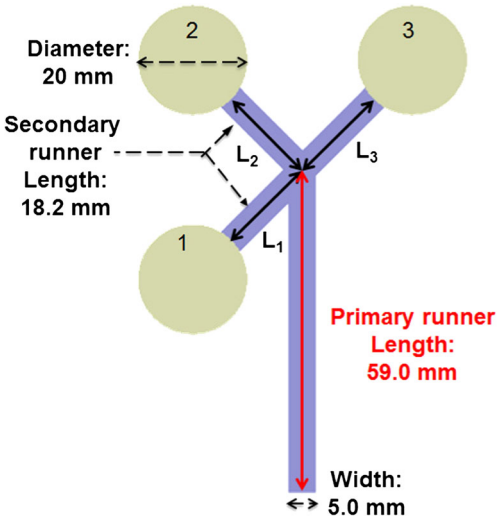

Fig. 1 Geometry and its dimensions of the model

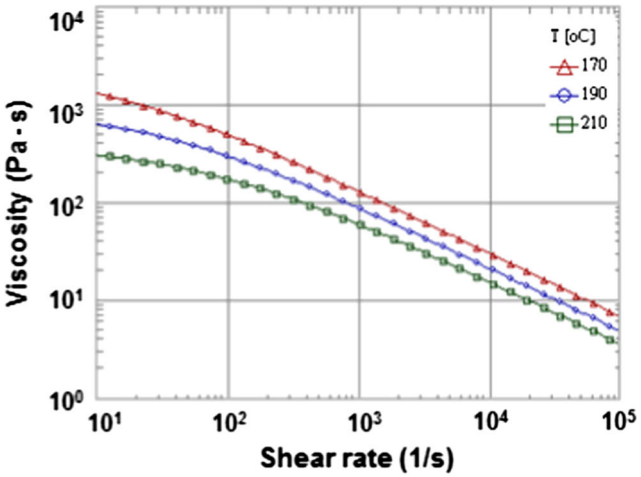

(a)

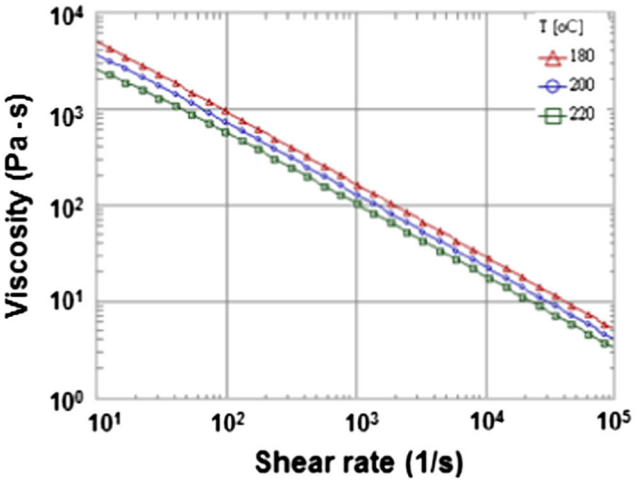

(b)

Fig. 2 The viscosity property against shear rate at various temperatures for **a** low viscosity material: GPPS Polyrex PG-22 (Chi-Mei) and **b** high viscosity material: GPPS Polyrex PG-383 (Chi-Mei)

Table 1 Process condition settings

Filling time	0.60 (sec)
Melt temperature	220.0 (°C)
Mold temperature	60.0 (°C)
Maximum injection pressure	250.0 (MPa)
Material	GPPS POLYREX PG-22 GPPS_POLYREXPG-383
Packing time	5 (sec)
Packing pressure	175.0 (MPa)
Mold opening time	5.0 (sec)
Ejection temperature	97.0 (°C)
Air temperature	25.0 (°C)
Core enter time (by volume filled)	72 (%)

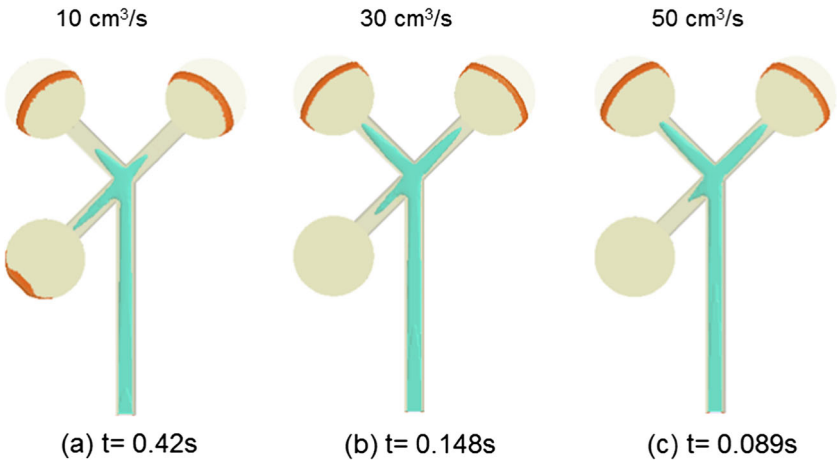

Fig. 3 The flow rate influence on the core penetration in the runner-filling stage at a fixed skin-to-core ratio of 72/28 using a low viscosity material system (GPPS Polyrex PG-22): the flow rates from (**a**) 10 cm^3/s to (**c**) 50 cm^3/s

is expected that the design of this bifurcation structure will influence the flow behavior which ultimately affects the skin-to-core distribution result. However, the detailed mechanism of how the bifurcation structure influences the core distribution of the final product is still unclear. On the other hand, an imbalanced filling behavior is a common problem in multi-cavity molding, even for a geometrically balanced multi-cavity runner system. When an imbalanced filling occurs between different cavities, inter-cavity variation or intra-cavity variation is most likely to happen. And, for a non-geometrically balanced multi-cavity runner system, the flow imbalance issue becomes more complicated [16–20].

Therefore, the purpose of this study is twofold. First, it is to understand the core material penetration behavior in the runner with a bifurcation structure when it is at the fixed skin-to-core ratio [14] and how it is sensitive to different material selections and process conditions. Second, it is to study how we can improve the core distribution result with a better inter-cavity balance through a suitable skin-to-core ratio adjustment and a proper control of process conditions under the geometric restrictions of a bifurcation runner design.

The details of this paper are organized as follows. The theory and assumption are illustrated in Section 2. In Section 3, we will show the detailed model and the related information. Then, the experiment results and discussion are addressed in Section 4, and Section 5 will be the conclusion.

1.1 Theory and assumption

The polymer melt is assumed as General Newtonian Fluid (GNF). Hence, the non-isothermal 3D flow motion can be mathematically described by the following:

$$\frac{\partial \rho}{\partial t} + \nabla\cdot\rho\mathbf{u} = 0 \tag{1}$$

$$\frac{\partial}{\partial t}(\rho\mathbf{u}) + \nabla\cdot(\rho\mathbf{u}\mathbf{u} - \boldsymbol{\sigma}) = \rho\mathbf{g} \tag{2}$$

$$\boldsymbol{\sigma} = -p\mathbf{I} + \eta\left(\nabla\mathbf{u} + \nabla\mathbf{u}^T\right) \tag{3}$$

$$\rho C_P\left(\frac{\partial T}{\partial t} + \mathbf{u}\cdot\nabla T\right) = \nabla\cdot(k\nabla T) + \eta\dot{\gamma}^2 \tag{4}$$

where $\mathbf{u}$ is the velocity vector, T is the temperature, t is the time, p is the pressure, $\boldsymbol{\sigma}$ is the total stress tensor, ρ is

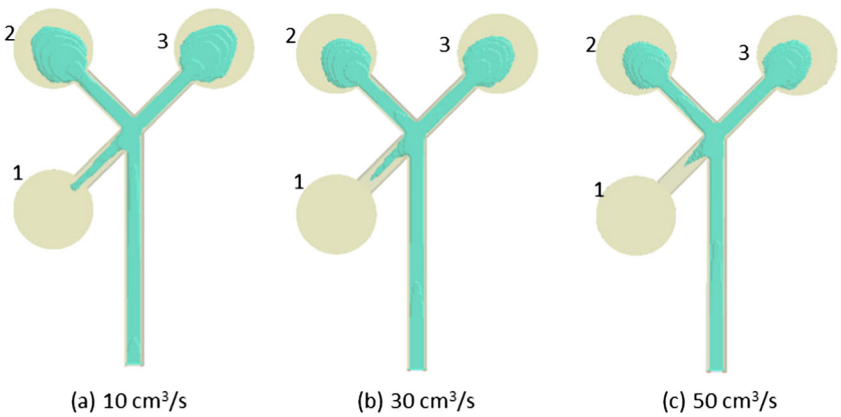

Fig. 4 The flow rate influence on the core penetration at the end of filling at a fixed skin-to-core ratio of 72/28 using a low viscosity material (GPPS Polyrex PG-22): the flow rates from (**a**) 10 cm^3/s to (**c**) 50 cm^3/s

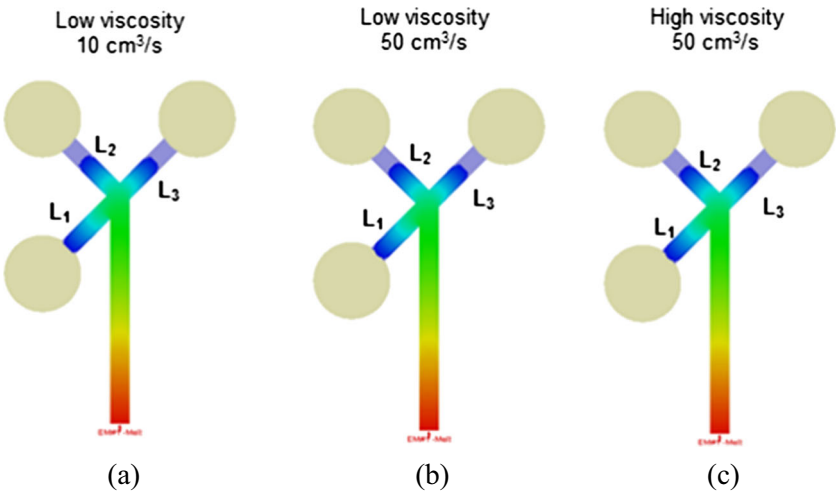

Fig. 5 The melt flow behaviors at various conditions. **a** A low viscosity material (GPPS Polyrex PG-22) at 10 cm^3/s. **b** A low-viscosity material (GPPS Polyrex PG-22) at 50 cm^3/s. **c** A high viscosity material (GPPS Polyrex PG-383) at 50 cm^3/s

the density, η is the viscosity, k is the thermal conductivity, C_p is the specific heat, and γ is the generalized shear rate. The Finite Volume Method (FVM) due to its robustness and efficiency is employed in this study to solve the transient flow field in a complex three-dimensional geometry [21]. In this work, the Modified-Cross model with Arrhenius temperature dependence is employed to describe the viscosity of polymer melt:

$$\eta(T,\gamma) = \frac{\eta_o(T)}{1 + (\eta_o\gamma/\tau^*)^{1-n}} \tag{5}$$

with

$$\eta_o(T) = \mathrm{BExp}\left(\frac{T_b}{T}\right) \tag{6}$$

where η is the viscosity, η_o is the zero shear viscosity, n is the power law index, B is called the consistency index, and τ^* is the parameter that describes the transition region between zero shear rate and the power law region of the viscosity curve.

To track the advancement of the interface position in the co-injection molding, a volume fractional function f is defined to describe the filling status of each cell. The fractional volume function is governed by the following transport equation:

$$\frac{\partial}{\partial t} f_i + \mathbf{u}\cdot\nabla f_i = 0 \tag{7}$$

Two transport equations for skin and core materials are solved to determine the advancement of interfaces and subscript i denotes for different transported material. For $i = 1$, the transported material is skin layer, where $f_1 = 1$ is defined as the cell filled by the skin polymer melt, $f_1 = 0$ as the empty cell enclosed by air; For $i = 2$, the transported material is core material, where $f_2 = 1$ defines as the cell filled by the core material, $f_2 = 0$ as the empty cell enclosed by air or skin material. Hence, the interfaces (skin/core, skin/gas, core/air) are located within the cells with $0 < f_i < 1$.

2 Model and related information

Figure 1 presents the geometry and the runner and cavity dimensions of the model. The diameter of each cavity is 20 mm with 3.5 mm in thickness. The length of the primary runner (before the bifurcation structure) is 59 mm. The length of the secondary runners (after the bifurcation structure) is 18.2 mm. In this study, the materials used are GPPS_POLYREXPG-22 for low viscosity (melt flow rate is 18.0 (g/10 min)) and GPPS_POLYREXPG-383 for high viscosity (melt flow rate is 2.2 (g/10 min)). The viscosity properties of these two materials are listed in Fig. 2. The general process condition settings are given in Table 1, including the filling time, the mold temperature, the melt temperature, the packing time, and so on. Specifically, the skin-to-core ratio is kept as 72/28; that is, when the total injected volume reaches 72% full, the gate for injecting the skin material will be closed and that of the core material will be open to allow the core material to flow through the runners into the cavities. Also, the material used for the skin and core in this study is the same material for each co-injection shot.

Furthermore, the numerical simulation is performed using the commercial CAE software, Moldex3D R13® to help analyze the intricate mechanism of the skin/core material flow behaviors. The experimental validation is also performed after the simulation study is done. In addition, we assign the numbers 1, 2, and 3 to each runner after the bifurcation as shown in Fig. 1 for identity purpose.

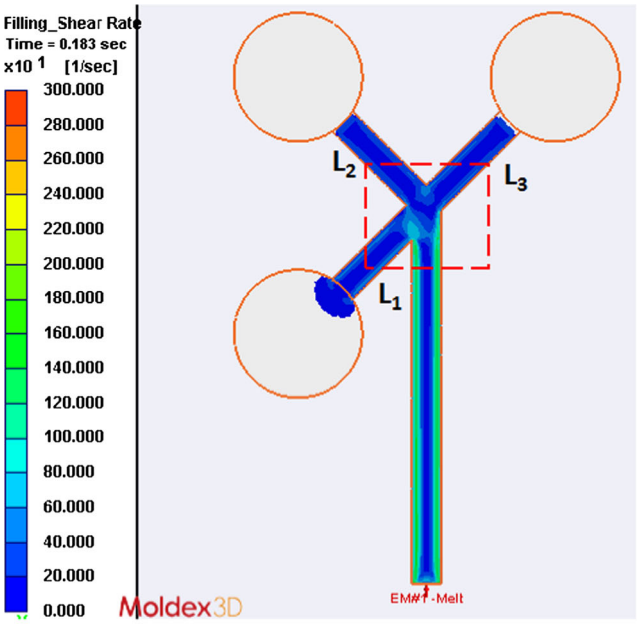

(a)

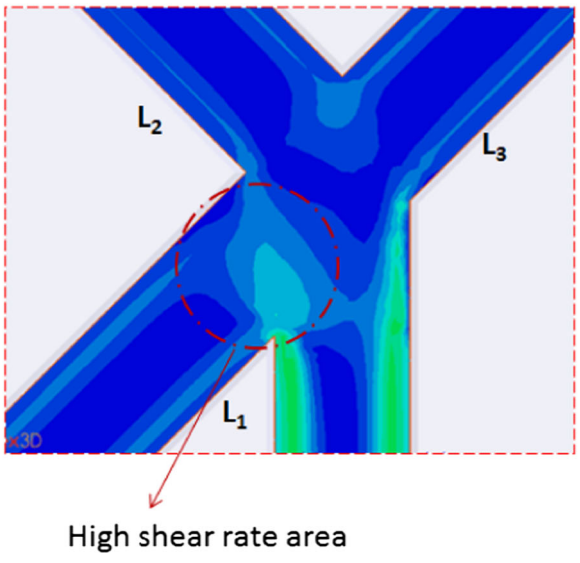

(b)

Fig. 6 **a** The shear rate distribution of a single shot using GPPS Polyrex PG-22 at 10 cm^3/s. **b** The high shear rate area

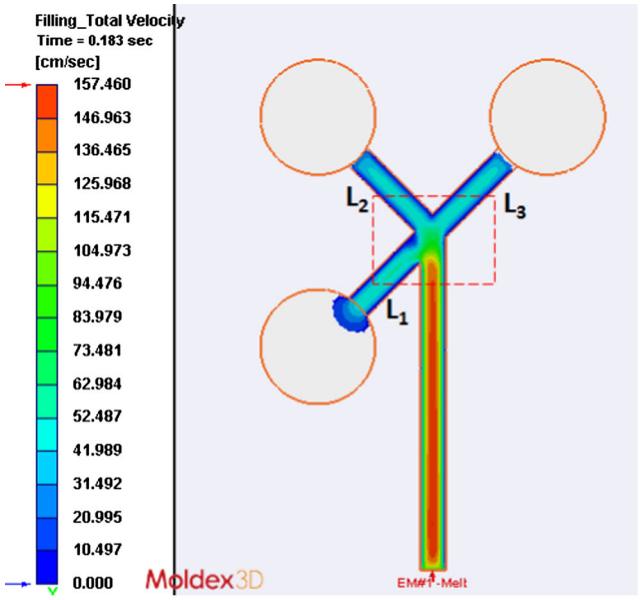

(a)

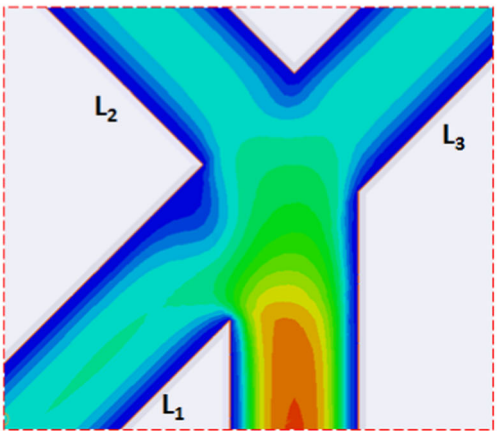

(b)

Fig. 7 **a** The total velocity distribution of a single shot with GPPS Polyrex PG-22 at 10 cm^3/s. **b** the total velocity distribution around the high shear rate area

3 Results and discussion

3.1 Core penetration and distribution prediction by numerical simulation

Figure 3 shows the flow rate influence on the core penetration at the runner-filling stage at a fixed skin-to-core ratio of 72/28 using a low viscosity material (GPPS Polyrex PG-22) from the flow rates of 10 to 50 cm^3/s. Clearly, when the flow rate is at 10 cm^3/s as shown in Fig. 3a, the core material reaches the end of runner L_1 first. When the flow rate is increased to 30 cm^3/s and higher as shown in Fig. 3b, c, the core material behavior will start to change and it will reach the end of runner L_2 first. This observation is the same as Yang and Yokois' in [14]. Figure 4 shows the core penetration results at the end of filling. The interesting thing is that although the flow rate seems to affect the core penetration at the runner-filling stage, however, it has no significant influence on improving the core material distribution of the final product. The final core penetration imbalance among different cavities cannot be altered at the end of filling, especially with a major problem in Cavity 1 where there is almost no core material inside the cavity. Comparing the differences between Cavity 1 and Cavity 2, or Cavity 1 and Cavity 3, it shows that the inter-cavity balance is very poor based on the core material distribution observation. This inter-cavity imbalance does not seem that it can

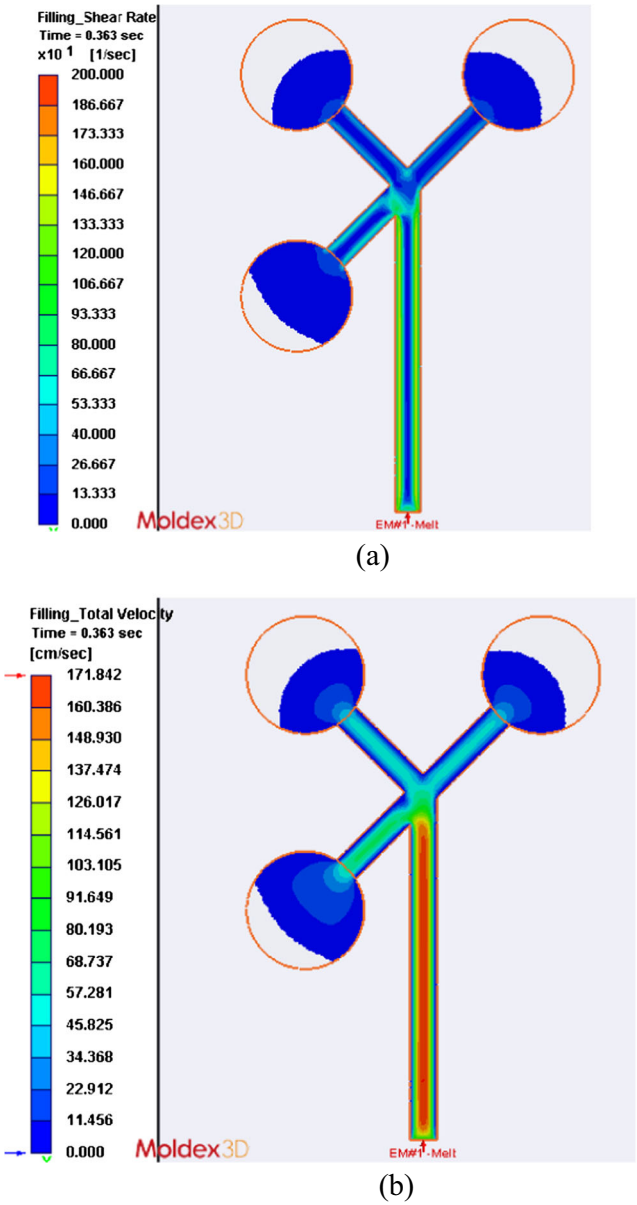

Fig. 8 **a** The shear rate distribution of a co-injection system with GPPS Polyrex PG-22 at 10 cm^3/s. **b** The total velocity distribution of a co-injection system with GPPS Polyrex PG-22 at 10 cm^3/s

be improved merely by changing various process conditions, such as melting temperature, mold temperature, or even replacing by a high-viscosity material: GPPS PG-383.

In the following sections, in order to understand the internal mechanism as to why the flow rate have a more direct impact on the core penetration behavior at the runner-filling stage but has no significant impact on the final core penetration result at the end of filling when it is at a fixed skin-to-core ratio of 72/28 and also to propose an effective method to overcome the poor inter-cavity balance problem, we first studied the melt flow behavior in single material injection molding, and then in co-injection molding next.

3.1.1 The melt flow behavior through single shot injection molding

Figure 5a and b show the melt flow behaviors through single shot injection molding. Even when the flow rate is changed from 10 cm^3/s to 50 cm^3/s, the melt still goes through runner L_1 and then fill Cavity 1 completely first. Moreover, in Fig. 5c, when the material is changed to GPPS PG-383, the flow behavior remains the same pattern as that of a low viscosity. Therefore, we could conclude that the flow rates and plastic materials do not have a direct impact on altering the flow behavior during the runner-filling stage in the multi-cavity design.

To further understand the internal mechanism of this flow behavior, we then studied the relationship between the shear rate and the total velocity. Figure 6a, b display the shear rate distribution of a single shot using GPPS PG-22 at 10 cm^3/s. In Fig. 6b, there is a high shear rate area observed in the bifurcation region toward L_1 where the shear rate is higher than other areas with 200–400 s^{-1}. Hence, when the melt passes through the bifurcation region, the high shear in the area will further reduce the melt viscosity and provide a higher total velocity as shown in Fig. 7a, b. It explains the reason why the melt generally goes through runner L_1 and then fill Cavity 1 completely first in a single shot injection molding. In a subsequent experiment, we applied a high flow rate of 50 cm^3/s with a different material: GPPS PG-383; the shear rate distribution and total velocity behavior show a similar trend.

3.1.2 The skin and core material flow behaviors through co-injection injection molding

Figure 8a shows the shear rate distribution at 72% of the total volume when the core material is about to enter the runners. At this point, the shear rate distribution and the high shear rate area observed at the bifurcation of the runner toward L_1 are very similar to those of single shot injection molding. The high shear rate will continuously provide a higher total velocity in the bifurcation of L_1 (as shown in Fig. 8b) to promote a faster filling in L_1 until Cavity 1 is completely filled. This inference can be further verified numerically as shown in Fig. 9. For a bifurcation runner structure in a multi-cavity co-injection system, the leading core flow front behavior is strongly dependent on the shear rate distribution in the runner region. That is, the leading core penetration will occur in the higher shear rate area in L_1 until Cavity 1 is fully filled. This leading core material phenomenon in L_1 would result in a poor inter-cavity balance of core distribution among different cavities. However, the overall flow mechanism at

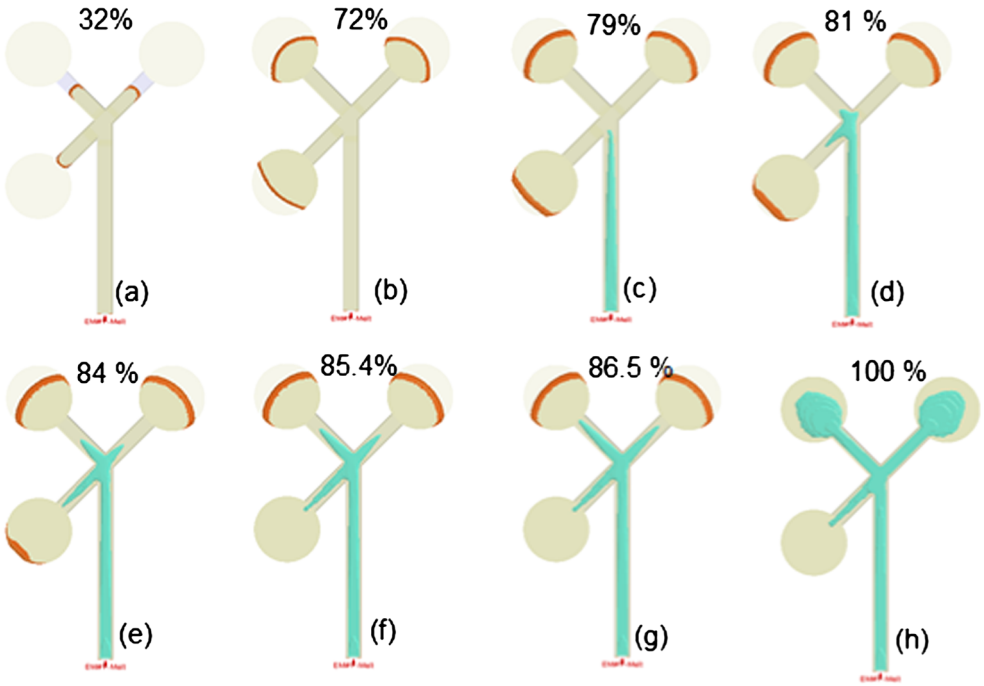

Fig. 9 Flow behavior of the core penetration using a low viscosity (GPPS Polyrex PG-22) at a low flow rate of 10 cm^3/s with various total volume ratios. **a** At 32%, the skin material reaches the cavity first. **b** At 72%, the core material begins to enter the runner. **d**–**h** Show the core material flow behaviors from 81% to the end of filling

a fixed skin-to-core ratio is the same as that of the single shot system.

3.1.3 Discover the flow rate influence on core penetration

Moreover, let us discover the flow rate influence on core penetration during the runner-filling stage and at the end of filling. Figure 10a, b show the slicing of the runner at the cross section in order to observe the skin and core penetrations at different velocities. The black color represents the volume space occupied by the core material. Basically, the core penetration velocities are perpendicular to the flow direction including $\langle V_Z \rangle$ and $\langle V_x \rangle$. In Fig. 10b, when the flow rate is increased from 10 to 50 cm^3/s, the core material will occupy more volume space in the upstream portion of the runner (i.e., the primary runner). The reason is that when the flow rate is increased, the same amount of melt enters the runner with lower resistance from the cold mold boundary, and then the core material can penetrate into the cross section directions in $\langle V_Z \rangle$and $\langle V_x \rangle$ much easily. In addition, Table 2 shows the related information to verify this phenomenon. As the skin material enters into the runners till 72% of total volume (t_1: it is the time required to finish the filling of skin and the beginning of core material entering the mold), the flow behavior is exactly the same as that of single shot injection molding. At this point, the cross velocity $\langle V_Z \rangle$ will be increased from 18 to 48 cm/s when the flow rate increases from 10 to 50 cm^3/s as well as the cross velocity $\langle V_x \rangle$, increasing from 59 to 250 cm/s. After this time step, the core material will enter into the runner until it reaches the end of the runner and the time required for this period is t_2. At this time step, the cross velocity $\langle V_Z \rangle$ will be increased from 20 to 51 cm/s when the flow rate increases from 10 to 50 cm^3/s as well as the cross velocity $\langle V_x \rangle$, increasing from 62 to 248 cm/s. After this time step, the core material continues to travel through runners and fill Cavity 1 completely first, and then it will switch to fill Cavity 2 and 3. For a fixed volume ratio of core material, when the flow rate is increased, the penetration in the cross-section directions will be increased, and the core penetration length will be reduced in the flow direction.

3.1.4 The proposal to improve the poor inter-cavity balance problem

As shown in Fig. 4, when we performed the multi-cavity co-injection system with a bifurcation runner at a fixed skin-to-core ratio of 72/28, the end result was a very poor inter-cavity balance with unsatisfactory core material distribution. To improve this imbalance issue, the manipulation of using different skin-to-core ratios can be quite useful. Figure 11 displays the various inter-cavity balance behaviors using different skin-to-core ratios with GPPS PG-22 at the flow rate of 10 cm^3/s. When the skin-to-core ratio is greater than 70/30, the core material never reaches Cavity 1. Therefore, a poor inter-cavity balance with unsatisfactory core material distribution will occur. In addition, when the skin-to-core ratio is decreased from 70/30 to 60/40, the core penetrated areas will be increased in all cavities. The inter-cavity imbalance problem will be

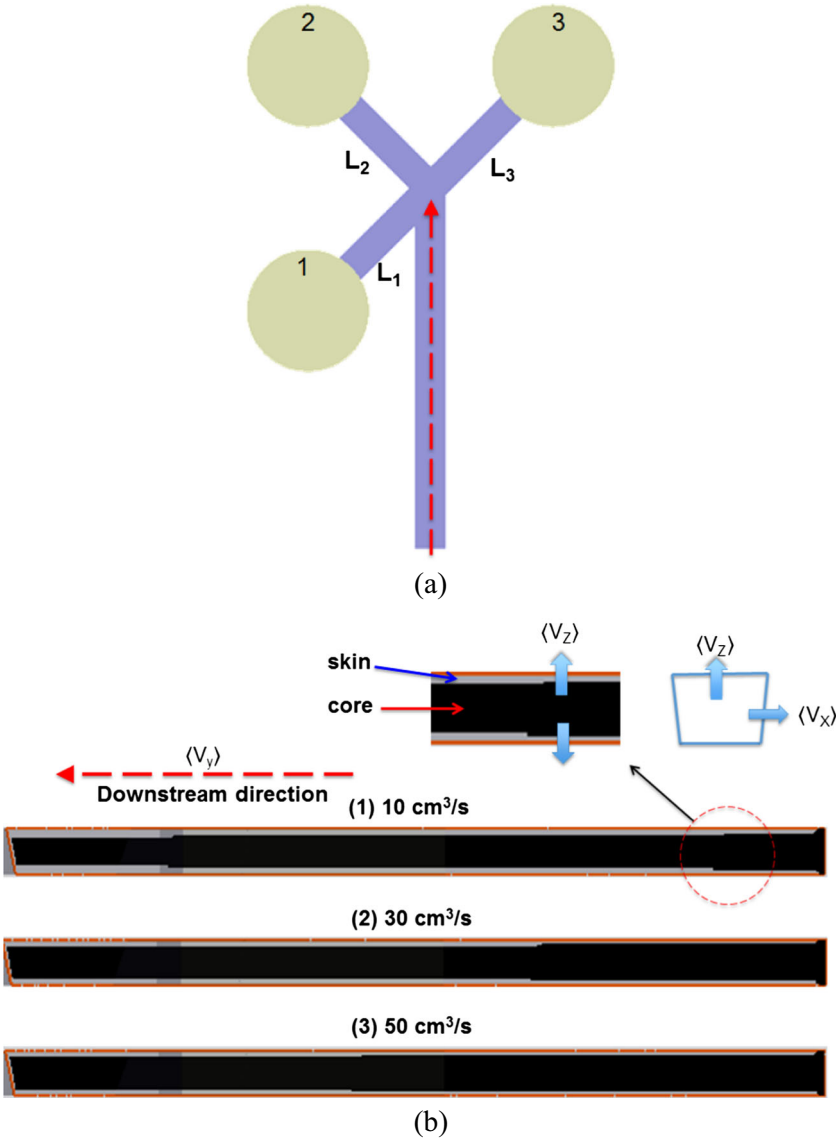

Fig. 10 Slicing the runner at the cross section. To observe the skin and core penetrations at different velocities, **a** the direction to make the slicing at the cross section, **b** the volume space occupation of core material (*black color*), and the velocity at the cross section $\langle V_Z \rangle$and V_x

improved. When the skin-to-core ratio is decreased to 55/45, another "core break-through" problem will occur in Cavity 2 and 3. When the ratio is decreased substantially to 30/70, the core break-through problem becomes more serious in all cavities. Hence, we could observe that when the flow rate is at 10 cm^3/s, the best skin-to-core ratio is around 60/40.

On the other hand, as discussed in the earlier section, a higher flow rate will reduce the core penetration length in the flow direction. Thus, it can be used to optimize the core penetration and distribution. Figure 12 shows the different flow rate influences using GPPS PG-22 in co-injection at a fixed skin-to-core ratio of 55/45. When the flow rate is at 10 cm^3/s, the core break-through problem

Table 2 Flow rate influence and its velocity

Flow rate (cm^3/s)	t_1 (s)	t_2 (s)	Volume percentage filled at t_2 (%)	$\langle V_x \rangle$ at t_1 (cm/s)	$\langle V_x \rangle$ at t_2 (cm/s)	$\langle V_Z \rangle$ at t_1 (cm/s)	$\langle V_Z \rangle$ at t_2 (cm/s)
10	0.363	0.42	84	59	62	18	20
30	0.121	0.148	86.4	165	165	48	49
50	0.072	0.089	88.5	250	248	48	51

t_1 the time required to fill 72% volume of melt, t_2 the time required from the core material first enters into the runner to it reaches the end of runner, V_Z and V_x average velocity at cross direction (cm/s) (see Fig. 10b)

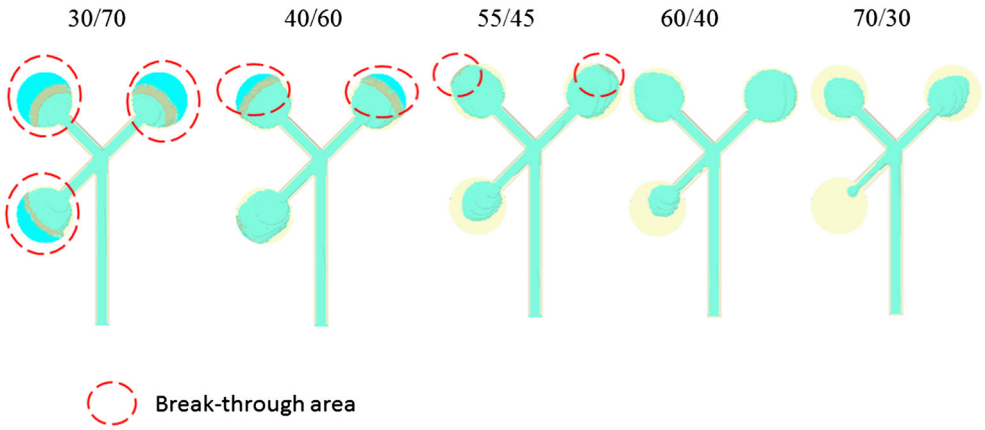

Fig. 11 The manipulation of using different skin-to-core ratios will change the inter-cavity balance but a core break-through problem may occur when an improper skin-to-core ratio is used

will occur in Cavity 2 and 3. As the flow rate is increased to 50 cm^3/s, the core penetration length will be reduced and the inter-cavity imbalance can be improved. Hence, through a suitable adjustment of the skin-to-core ratio, and a proper control of the flow rate, a reasonable inter-cavity balance with satisfactory core distribution in multi-cavity molding with a bifurcation runner design can be achieved.

3.2 Experimental validation

In order to validate our inference using the numerical simulations and the effectiveness of our proposal to improve the inter-cavity imbalance and core break-through problem, we performed a series of experimental studies as follows.

1. The melt flow behavior through single shot injection molding

Figure 13 shows a short shot testing for single shot injection molding using GPPS PG-22 at the flow rate of 10 cm^3/s. Clearly, the melt travels through runner channel L_1 predominantly and fill Cavity 1 completely first before it moves to fill Cavity 2 and 3. Experimental results are consistent with our simulation predictions.

2. The skin and core material flow behaviors through co-injection injection molding

Figure 14 shows a short shot testing for co-injection molding using GPPS PG-22 at a fixed skin-to-core ratio of 72/28 and at the flow rate of 10 cm^3/s. Clearly, the melts including both the skin and core materials go through runner channel L_1 predominately and fill Cavity 1 completely first before they move to fill Cavity 2 and 3. Experimental results validated our simulation analyses.

3. Discover the flow rate influence on core penetration

Figure 15 exhibits the different core penetration behaviors when the flow rate is increased from 10 to 50 cm^3/s. At a higher flow rate, the core material will occupy more volume space in the upstream portion of the runner, and

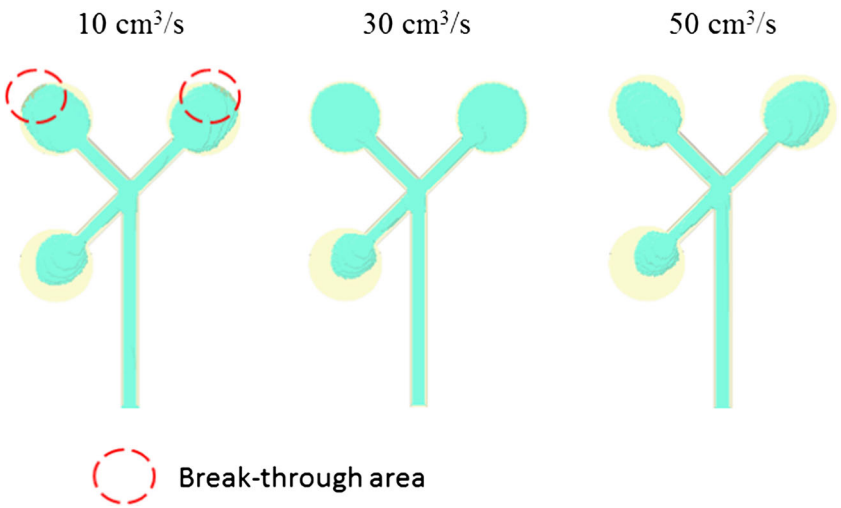

Fig. 12 At a fixed skin-to-core ratio of 55/45, using a high flow rate of 50 cm^3/s can prevent the core break-through problem encountered in a lower flow rate system (10 cm^3/s); thus, the inter-cavity balance can be improved

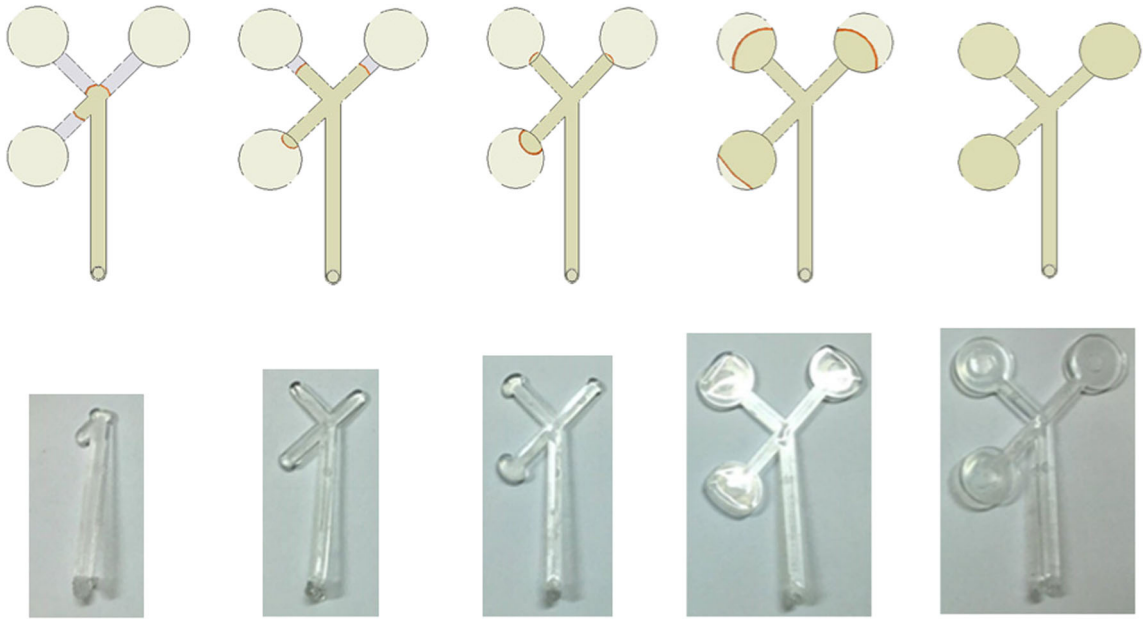

Fig. 13 Experiment validation for a single material (skin layer) filling in a low viscosity material system (GPPS Polyrex PG-22) at the flow rate of 10 cm^3/s

then the penetration distance will be reduced in the flow direction. Both numerical predictions and experimental results are in reasonably good agreement.

4. The proposal to improve the poor inter-cavity balance problem

Lastly, we proposed to modify the skin-to-core ratio and increase the flow rate to improve the poor inter-cavity balance problem and prevent the core break-through defect from happening. Figure 16 shows the experiment validation for the skin-to-core ratio of 55/45 with a low viscosity material system (GPPS Polyrex PG-22). In Fig. 16a, the core break-through occurs at 10 cm^3/s. In Fig. 16b, c, the increased flow rates can prevent the core break-through defect from happening and also improve the inter-cavity balance. The experimental data verified the feasibility of our proposal.

4 Conclusion

In this study, it has focused on studying the multi-cavity co-injection system with a bifurcation runner structure. The conclusions are as follows.

1. When the skin-to-core ratio is fixed (say 72/28), the non-symmetrical bifurcation runner structure will lead to a higher shear rate in the bifurcation area where the shear rate difference will further induce the total velocity difference among different runners. Consequently, it will cause the imbalance of core distribution between the cavities. This inter-cavity imbalance problem will still persist even if the melt temperature, the mold temperature, or the plastic material is modified. However, when the flow rate is increased, the core material will occupy more volume space in the upstream portion of the runner and then the penetration distance will be reduced in the flow direction downstream. This feature is very useful to further manipulate the skin/core interface in a multi-cavity system.
2. Regarding how to improve a poor inter-cavity balance with unsatisfactory core material distribution, a suitable adjustment of the skin-to-core ratio is very useful. However, the core break-through defect can be a common problem when an unsuitable skin-to-core ratio is used. To prevent the core break-through defect from happening, a proper increase of the flow rate is one of the good options. Hence, we could conclude that through a suitable adjustment of the skin-to-core ratio and a proper flow rate control, we can optimize the core material distribution in multi-cavity co-injection system with a bifurcation runner structure.
3. In order to validate our inference and the effectiveness of our proposal to improve the inter-cavity imbalance and prevent the core break-through problem, we also performed a series of experimental studies. The studies included the testing of the melt flow behavior through single shot injection molding, the verification

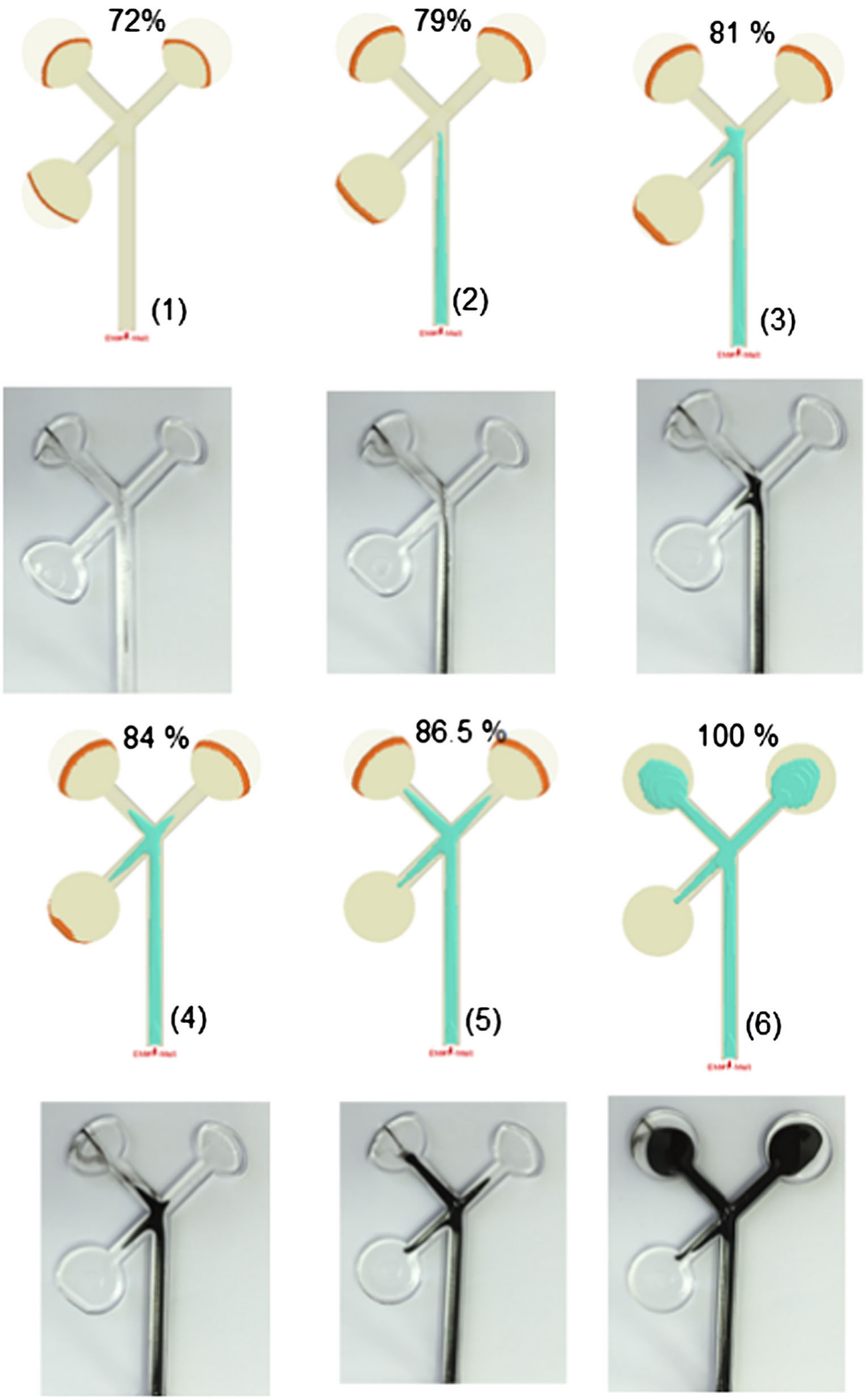

Fig. 14 Experiment validation for both skin and core fillings at a fixed skin-to-core ratio of 72/28 in a low viscosity material system (GPPS Polyrex PG-22) at the flow rate of 10 cm^3/s

of the skin and core material flow behaviors through co-injection injection molding, and the flow rate influence on the core penetration. We were able to verify the feasibility of our proposal on improving the poor inter-cavity balance problem and the core break-through defect.

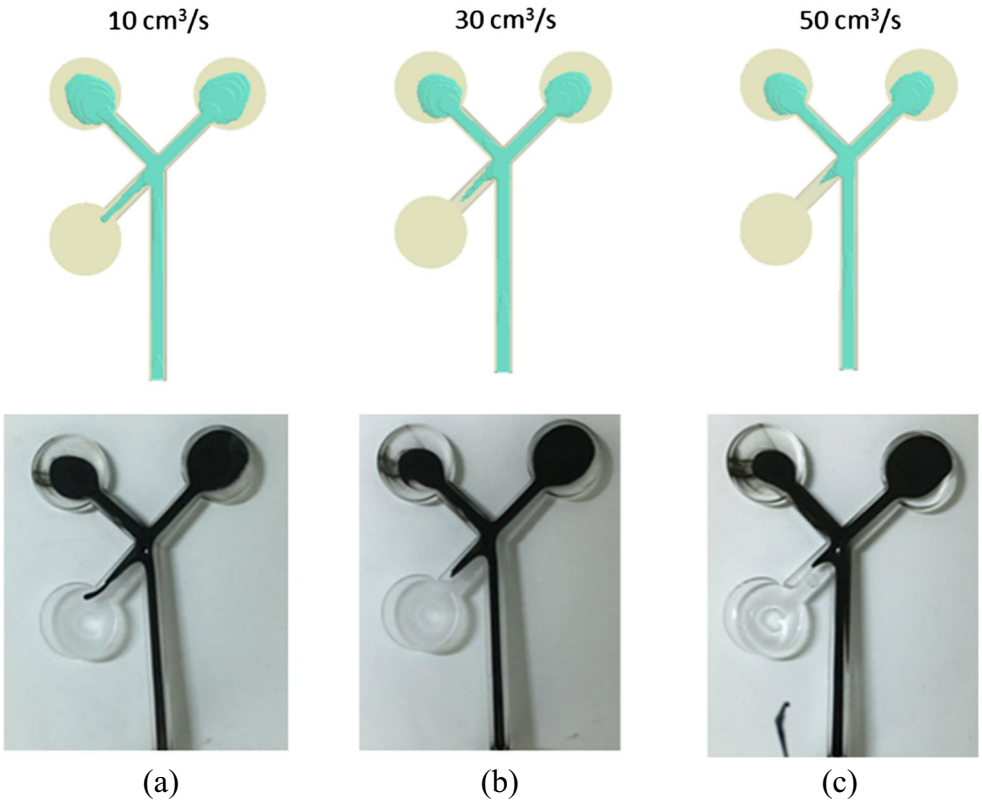

Fig. 15 Experiment validation for both skin and core fillings at a skin-to-core ratio of 72/28 in a low viscosity material system (GPPS Polyrex PG-22): the flow rates are increased from 10 to 50 cm^3/s

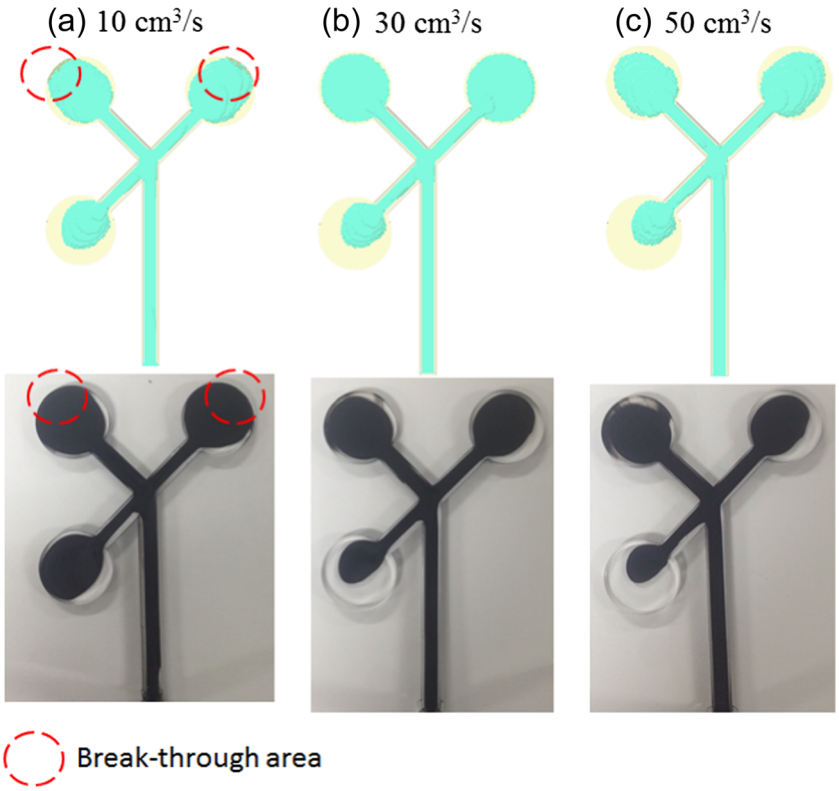

Fig. 16 Experiment validation for a skin-to-core ratio of 55/45 in a low viscosity material system (GPPS Polyrex PG-22). **a** the core break-through problem occurs at 10 cm^3/s. **b** the core break-through problem is gradually improved from 30 cm^3/s. **c** the core break-through problem is prevented and the inter-cavity imbalance is improved

Acknowledgements I would like to thank Ministry of Science and Technology of Taiwan, Republic of China (Project number: MOST 105-2218-E-032-002-) for their financial support of this research. I also would like to thank Ms. Jackie Yang and Mr. Kuan-Hao Chen for their assistance in the preparations of the simulation information. Additionally, my special gratitude goes to Dr. Rong-Yeu Chang and CoreTech System Co. for their continuous technical support. Lastly, a special thanks to Prof. Shi-Chang Tseng and Mr. Pin-Ju Huang for providing the experimental data.

References

1. Foss PH, Tseng H-C, Snawerdt J, Chang Y-J, Yang W-H, Hsu C-H (2014) Prediction of fiber orientation distribution in injection molded parts using Moldex3D simulation. Polym Compos 35(4): 671–680
2. Thomason JL, Vlug MA (1996) Influence of fiber length and concentration on the properties of glass fiber-reinforced polypropylene: Part 1-Tensile and flexural modulus. Composites 27A:477–484
3. Tseng H-C, Chang R-Y, Hsu C-H (2013) Phenomenological improvements to predictive models of fiber orientation in concentrated suspensions. J Rheol 57:1597
4. Composites World (2014) Website information: http://www.compositesworld.com/articles/recycled-carbon-fiber-update-closing-the-cfrp-lifecycle-loop, Accessed: Sep. 14, 2015
5. Job S (2014) Recycling composites commercially. Reinforced Plastics 32–38
6. Pimenta S, Pinho ST (2011) Recycling carbon fibre reinforced polymers for structural applications: technology review and market outlook. Waste Manag 31:378–392
7. Garner PJ, Oxley DF (1969) Process for the production of cellular articles. British Patent 1,156,217
8. Goodship V, Love JC (2002) Multi-material injection molding. Rapra Review Reports 145(13):1–31
9. Gomes M, Martino D, Pontes AJ, Viana JC (2011) Co-injection molding of immiscible polymers: skin-core structure and adhesion studies. Polymer engineering science 51(12):2398–2407
10. Messaoud D, Sanchagrin B, Derdouri A (2005) Study on mechanical properties and material distribution of sandwich plaques molded by co-injection. Polym Compos 26(3):265–275
11. Sun SP, Hsu CC, Huang CT et al (2012) The skin/core material distribution of a co-injection molding process: the effect of processing conditions and material selection, SPE ANTEC Tech Paper, Paper No. 1258422
12. Liu Q, Ouyang J, Zhou W, Xu X, Zhang L (2015) Numerical simulation of the sequential coinjection molding process based on level set method. Polymer and Engineering Science 55(8):1709–1019
13. Huang C-T, Yang J, Chang R-Y (2015) Dynamic penetration behavior of core-material in multi-cavity co-injection molding. AIP Conference Proceedings 1695:020002-1-8
14. Yang WM, Yokoi H (2003) Visual analysis of the flow behavior of core material in a fork portion of plastic sandwich injection moulding. Polym Test 22:37–43
15. Thomas Technik + Innovation (2016) Website information: http://www.thomas-technik.de/en/bedsystems.htm, Accessed: Aug. 10, 2016
16. Beaumont JP, Young JH (1997) Mold filling imbalances in geometrically balanced runner systems. Journal of Injection Molding Technology 1(3):133–144
17. Beaumont JP (2001) Beaumont runner technologies, Inc. "Intracavity filling imbalances" Technical Brief
18. Beaumont JP (2004) Runner and gating design HandBook, (2nd ed, Hanser, Munich), pp 63–110
19. Chien JC, Huang CT, Yang WH et al (2006) True 3D CAE visualization of intra-cavity filling imbalance in injection. SPE ANTEC Tech. Paper 1153–1157
20. Chien CC, Peng YH, Yang WL et al (2007) Effects of melt rotation on Warpage phenomena in injection molding. SPE ANTEC Tech. Paper 572–576
21. Chang RY, Yang WH (2001) Numerical simulation of mold filling in injection molding using a three-dimensional finite volume approach. Int J Numer Meth Fluids 37:125–148